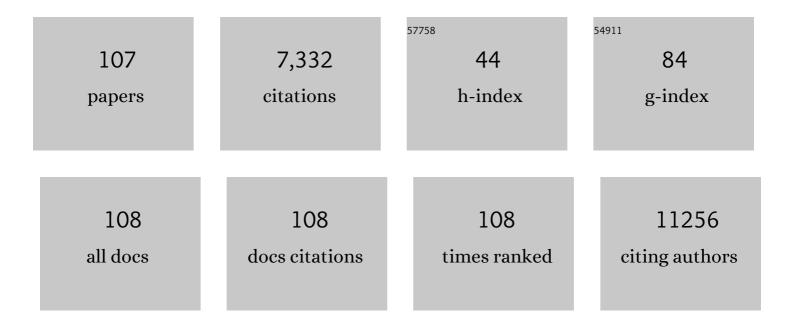
Zhenpeng Hu

List of Publications by Year in descending order

Source: https://exaly.com/author-pdf/6448208/publications.pdf Version: 2024-02-01



#	Article	IF	CITATIONS
1	Engineering surface atomic structure of single-crystal cobalt (II) oxide nanorods for superior electrocatalysis. Nature Communications, 2016, 7, 12876.	12.8	568
2	Activating cobalt(II) oxide nanorods for efficient electrocatalysis by strain engineering. Nature Communications, 2017, 8, 1509.	12.8	361
3	CO2 methanation on Ru-doped ceria. Journal of Catalysis, 2011, 278, 297-309.	6.2	328
4	Engineering electrocatalytic activity in nanosized perovskite cobaltite through surface spin-state transition. Nature Communications, 2016, 7, 11510.	12.8	316
5	Chemistry of Lewis Acid–Base Pairs on Oxide Surfaces. Journal of Physical Chemistry C, 2012, 116, 10439-10450.	3.1	293
6	Choice of <i>U</i> for DFT+ <i>U</i> Calculations for Titanium Oxides. Journal of Physical Chemistry C, 2011, 115, 5841-5845.	3.1	264
7	Single Mo ₁ (Cr ₁) Atom on Nitrogen-Doped Graphene Enables Highly Selective Electroreduction of Nitrogen into Ammonia. ACS Catalysis, 2019, 9, 3419-3425.	11.2	258
8	General Ï€â€Electronâ€Assisted Strategy for Ir, Pt, Ru, Pd, Fe, Ni Singleâ€Atom Electrocatalysts with Bifunctional Active Sites for Highly Efficient Water Splitting. Angewandte Chemie - International Edition, 2019, 58, 11868-11873.	13.8	229
9	Atomically and Electronically Coupled Pt and CoO Hybrid Nanocatalysts for Enhanced Electrocatalytic Performance. Advanced Materials, 2017, 29, 1604607.	21.0	224
10	Methane complete and partial oxidation catalyzed by Pt-doped CeO2. Journal of Catalysis, 2010, 273, 125-137.	6.2	186
11	Supported Rhodium Catalysts for Ammonia–Borane Hydrolysis: Dependence of the Catalytic Activity on the Highest Occupied State of the Single Rhodium Atoms. Angewandte Chemie - International Edition, 2017, 56, 4712-4718.	13.8	173
12	Atomic-level structure engineering of metal oxides for high-rate oxygen intercalation pseudocapacitance. Science Advances, 2018, 4, eaau6261.	10.3	164
13	Mechanism for Negative Differential Resistance in Molecular Electronic Devices: Local Orbital Symmetry Matching. Physical Review Letters, 2007, 99, 146803.	7.8	150
14	Quadruple perovskite ruthenate as a highly efficient catalyst for acidic water oxidation. Nature Communications, 2019, 10, 3809.	12.8	150
15	The Crucial Role of Charge Accumulation and Spin Polarization in Activating Carbonâ€Based Catalysts for Electrocatalytic Nitrogen Reduction. Angewandte Chemie - International Edition, 2020, 59, 4525-4531.	13.8	149
16	Tunable Band Structures of Heterostructured Bilayers with Transition-Metal Dichalcogenide and MXene Monolayer. Journal of Physical Chemistry C, 2014, 118, 5593-5599.	3.1	147
17	Activating Titania for Efficient Electrocatalysis by Vacancy Engineering. ACS Catalysis, 2018, 8, 4288-4293.	11.2	141
18	Rational Design of Spinel Cobalt Vanadate Oxide Co ₂ VO ₄ for Superior Electrocatalysis. Advanced Materials, 2020, 32, e1907168.	21.0	134

#	Article	IF	CITATIONS
19	A Dualâ€Stimuliâ€Responsive Coordination Network Featuring Reversible Wideâ€Range Luminescenceâ€Tuning Behavior. Angewandte Chemie - International Edition, 2019, 58, 5614-5618.	13.8	132
20	Realization of flat band with possible nontrivial topology in electronic Kagome lattice. Science Advances, 2018, 4, eaau4511.	10.3	131
21	Effect of Dopants on the Energy of Oxygen-Vacancy Formation at the Surface of Ceria: Local or Global?. Journal of Physical Chemistry C, 2011, 115, 17898-17909.	3.1	118
22	Synthetic paramontroseite VO2 with good aqueous lithium–ion battery performance. Chemical Communications, 2008, , 3891.	4.1	102
23	Chemistry of Doped Oxides: The Activation of Surface Oxygen and the Chemical Compensation Effect. Journal of Physical Chemistry C, 2011, 115, 3065-3074.	3.1	102
24	Chemical state of surrounding iron species affects the activity of Fe-Nx for electrocatalytic oxygen reduction. Applied Catalysis B: Environmental, 2019, 251, 240-246.	20.2	101
25	Pd–Pt Tesseracts for the Oxygen Reduction Reaction. Journal of the American Chemical Society, 2021, 143, 496-503.	13.7	100
26	The Quasiâ€Ptâ€Allotrope Catalyst: Hollow PtCo@singleâ€Atom Pt ₁ on Nitrogenâ€Doped Carbon toward Superior Oxygen Reduction. Advanced Functional Materials, 2019, 29, 1807340.	14.9	97
27	Strongly Coupled Nafion Molecules and Ordered Porous CdS Networks for Enhanced Visibleâ€Light Photoelectrochemical Hydrogen Evolution. Advanced Materials, 2016, 28, 4935-4942.	21.0	95
28	Synergistic Effect of Titanate-Anatase Heterostructure and Hydrogenation-Induced Surface Disorder on Photocatalytic Water Splitting. ACS Catalysis, 2015, 5, 1708-1716.	11.2	92
29	Band Gap Modulated by Electronic Superlattice in Blue Phosphorene. ACS Nano, 2018, 12, 5059-5065.	14.6	92
30	Ultrahigh Infrared Photoresponse from Core–Shell Singleâ€Đomainâ€VO ₂ /V ₂ O ₅ Heterostructure in Nanobeam. Advanced Functional Materials, 2014, 24, 1821-1830.	14.9	87
31	gt-C3N4 coordinated single atom as an efficient electrocatalyst for nitrogen reduction reaction. Nano Research, 2019, 12, 1181-1186.	10.4	87
32	Hexagonal Cu2SnS3 with metallic character: Another category of conducting sulfides. Applied Physics Letters, 2007, 91, .	3.3	85
33	Wellâ€Defined Singleâ€Atom Cobalt Catalyst for Electrocatalytic Flue Gas CO ₂ Reduction. Small, 2020, 16, e2001896.	10.0	85
34	Electronic and Magnetic Properties of Metal Phthalocyanines on Au(111) Surface: A First-Principles Study. Journal of Physical Chemistry C, 2008, 112, 13650-13655.	3.1	81
35	Tuning the catalytic property of nitrogen-doped graphene for cathode oxygen reduction reaction. Physical Review B, 2012, 85, .	3.2	81
36	Surface Nitrogen-Injection Engineering for High Formation Rate of CO ₂ Reduction to Formate. Nano Letters, 2020, 20, 6097-6103.	9.1	71

#	Article	IF	CITATIONS
37	Synergistic Effects between Doped Nitrogen and Phosphorus in Metal-Free Cathode for Zinc-Air Battery from Covalent Organic Frameworks Coated CNT. ACS Applied Materials & Interfaces, 2017, 9, 44519-44528.	8.0	65
38	Two-Dimensional Superlattice: Modulation of Band Gaps in Graphene-Based Monolayer Carbon Superlattices. Journal of Physical Chemistry Letters, 2012, 3, 3373-3378.	4.6	60
39	Dirac Signature in Germanene on Semiconducting Substrate. Advanced Science, 2018, 5, 1800207.	11.2	59
40	Quasi Chiral Phase Separation in a Two-Dimensional Orientationally Disordered System:Â 6-Nitrospiropyran on Au(111). Journal of the American Chemical Society, 2007, 129, 3857-3862.	13.7	57
41	A first-principles study on the electrochemical reaction activity of 3d transition metal single-atom catalysts in nitrogen-doped graphene: Trends and hints. EScience, 2022, 2, 219-226.	41.6	51
42	Metallic mesocrystal nanosheets of vanadium nitride for high-performance all-solid-state pseudocapacitors. Nano Research, 2015, 8, 193-200.	10.4	50
43	The origin of the enhanced photocatalytic activity of carbon nitride nanotubes: a first-principles study. Journal of Materials Chemistry A, 2017, 5, 4827-4834.	10.3	50
44	Halogen Adsorption on CeO ₂ : The Role of Lewis Acid–Base Pairing. Journal of Physical Chemistry C, 2012, 116, 6664-6671.	3.1	48
45	Kondo effect in single cobalt phthalocyanine molecules adsorbed on Au(111) monoatomic steps. Journal of Chemical Physics, 2008, 128, 234705.	3.0	44
46	Correlation-driven eightfold magnetic anisotropy in a two-dimensional oxide monolayer. Science Advances, 2020, 6, eaay0114.	10.3	43
47	V "Bridged―CoO to Eliminate Charge Transfer Barriers and Drive Lattice Oxygen Oxidation during Waterâ€Splitting. Advanced Functional Materials, 2021, 31, 2008822.	14.9	40
48	Hydrogen Treatment for Superparamagnetic VO ₂ Nanowires with Large Roomâ€Temperature Magnetoresistance. Angewandte Chemie - International Edition, 2016, 55, 8018-8022.	13.8	37
49	Construction of a polyhedron decorated MOF with a unique network through the combination of two classic secondary building units. Chemical Communications, 2016, 52, 2079-2082.	4.1	36
50	Imaging metal-like monoclinic phase stabilized by surface coordination effect in vanadium dioxide nanobeam. Nature Communications, 2017, 8, 15561.	12.8	33
51	Activating Inert Surface Pt Single Atoms via Subsurface Doping for Oxygen Reduction Reaction. Nano Letters, 2021, 21, 7970-7978.	9.1	33
52	Pt Atom on the Wall of Atomic Layer Deposition (ALD)â€Made MoS ₂ Nanotubes for Efficient Hydrogen Evolution. Small, 2022, 18, e2105129.	10.0	29
53	Hydrodebromination and Oligomerization of Dibromomethane. ACS Catalysis, 2012, 2, 479-486.	11.2	28
54	General Ï€â€Electronâ€Assisted Strategy for Ir, Pt, Ru, Pd, Fe, Ni Singleâ€Atom Electrocatalysts with Bifunctional Active Sites for Highly Efficient Water Splitting. Angewandte Chemie, 2019, 131, 11994-11999.	2.0	28

#	Article	IF	CITATIONS
55	STM characterization of size-selected V1, V2, VO, and VO2 clusters on a TiO2(110)-(1×1) surface at room temperature. Surface Science, 2011, 605, 972-976.	1.9	27
56	Supported Rhodium Catalysts for Ammonia–Borane Hydrolysis: Dependence of the Catalytic Activity on the Highest Occupied State of the Single Rhodium Atoms. Angewandte Chemie, 2017, 129, 4790-4796.	2.0	27
57	Auxetic two-dimensional transition metal selenides and halides. Npj Computational Materials, 2020, 6, .	8.7	27
58	Atomic Cobalt Vacancy luster Enabling Optimized Electronic Structure for Efficient Water Splitting. Advanced Functional Materials, 2021, 31, 2101797.	14.9	26
59	In situ unravelling structural modulation across the charge-density-wave transition in vanadium disulfide. Physical Chemistry Chemical Physics, 2015, 17, 13333-13339.	2.8	24
60	A Dualâ€Stimuliâ€Responsive Coordination Network Featuring Reversible Wideâ€Range Luminescenceâ€Tuning Behavior. Angewandte Chemie, 2019, 131, 5670-5674.	2.0	24
61	Observation of Hierarchical Chiral Structures in 8-Nitrospiropyran Monolayers. Journal of Physical Chemistry B, 2007, 111, 6973-6977.	2.6	23
62	Identifying atomic geometry and electronic structure of (2×3)-Sr/Si(100) surface and its initial oxidation. Journal of Chemical Physics, 2008, 129, 164707.	3.0	22
63	An amorphous tin-based nanohybrid for ultra-stable sodium storage. Journal of Materials Chemistry A, 2018, 6, 18920-18927.	10.3	22
64	Homogeneous-like Alkyne Selective Hydrogenation Catalyzed by Cationic Nickel Confined in Zeolite. CCS Chemistry, 2022, 4, 949-962.	7.8	20
65	The atomic structures of carbon nitride sheets for cathode oxygen reduction catalysis. Journal of Chemical Physics, 2013, 138, 164706.	3.0	19
66	Corrugation Matters: Structure Models of Single Layer Heptazine-Based Graphitic Carbon Nitride from First-Principles Studies. Journal of Physical Chemistry C, 2020, 124, 4644-4651.	3.1	19
67	Regular Arrangement of Two-Dimensional Clusters of Blue Phosphorene on Ag(111). Chinese Physics Letters, 2020, 37, 096803.	3.3	17
68	Ultrathin Van der Waals Antiferromagnet CrTe ₃ for Fabrication of Inâ€Plane CrTe ₃ /CrTe ₂ Monolayer Magnetic Heterostructures. Advanced Materials, 2022, 34, e2200236	21.0	17
69	xmlns:mml="http://www.w3.org/1998/Math/MathML"> <mml:msub><mml:mi>MoS</mml:mi><mml:mn>2using <mml:math xmlns:mml="http://www.w3.org/1998/Math/MathML"><mml:mrow><mml:msub><mml:mi< td=""><td>mn> 3.2</td><td>l:msub>15</td></mml:mi<></mml:msub></mml:mrow></mml:math </mml:mn></mml:msub>	mn> 3.2	l:msub>15
70	mathvariant="normal">G <mml:mn>O</mml:mn> <mml:msub><mml:msub><mml:mi mathvariant="normal">W<mml:mn>O</mml:mn></mml:mi </mml:msub></mml:msub> -BSE. Detecting a Moleculeâ^'Surface Hybrid State by an Fe-Coated Tip with a Non-s-Like Orbital. Journal of Physical Chemistry C, 2008, 112, 15603-15606.	3.1	14
71	The Key Role of van der Waals Interactions in MPc/Au(111) (M = Co, Fe, H ₂) Systems Based on First-Principles Calculations. Journal of Physical Chemistry C, 2014, 118, 27843-27849.	3.1	14
72	Electronic and geometric factors affecting oxygen vacancy formation on CeO2(111) surfaces: A first-principles study from trivalent metal doping cases. Applied Surface Science, 2019, 497, 143732.	6.1	14

#	Article	IF	CITATIONS
73	A promising way to open an energy gap in bilayer graphene. Nanoscale, 2015, 7, 17096-17101.	5.6	13
74	Screw dislocation-driven t-Ba ₂ V ₂ O ₇ helical meso/nanosquares: microwave irradiation assisted-SDBS fabrication and their unique magnetic properties. Journal of Materials Chemistry C, 2017, 5, 6336-6342.	5.5	13
75	Efficient energy gap tuning for T-carbon via single atomic doping. Chemical Physics, 2019, 518, 69-73.	1.9	13
76	Experimental Realization of Two-Dimensional Buckled Lieb Lattice. Nano Letters, 2020, 20, 2537-2543.	9.1	12
77	Identification of metal-cage coupling in a single metallofullerene by inelastic electron tunneling spectroscopy. Applied Physics Letters, 2010, 96, 253110.	3.3	9
78	DFT+ <i>U</i> Analysis on Stability of Low-Index Facets in Hexagonal LaCoO3 Perovskite: Effect of Co3+ Spin States. Chinese Journal of Chemical Physics, 2017, 30, 295-302.	1.3	9
79	Writing charge into the <i>n</i> -type LaAlO3/SrTiO3 interface: A theoretical study of the H2O kinetics on the top AlO2 surface. Applied Physics Letters, 2012, 101, .	3.3	8
80	Interactions in different domains of truxenone supramolecular assembly on Au(111). Physical Chemistry Chemical Physics, 2012, 14, 3980.	2.8	8
81	Growth and theoretical study on the deep-ultraviolet transparent β-CsBa ₂ (PO ₃) ₅ nonlinear optical crystal. CrystEngComm, 2019, 21, 4690-4695.	2.6	8
82	The Crucial Role of Charge Accumulation and Spin Polarization in Activating Carbonâ€Based Catalysts for Electrocatalytic Nitrogen Reduction. Angewandte Chemie, 2020, 132, 4555-4561.	2.0	8
83	Complex spin Hamiltonian represented by an artificial neural network. Physical Review B, 2022, 105, .	3.2	8
84	Passivating a transition-metal surface for more uniform growth of graphene: Effect of Au alloying on Ni(111). Physical Review B, 2013, 87, .	3.2	7
85	Efficient Method for Fast Simulation of Scanning Tunneling Microscopy with a Tip Effect. Journal of Physical Chemistry A, 2014, 118, 8953-8959.	2.5	7
86	Synthesis, structure and characterization of M(IO ₃) ₂ (HIO ₃) (M =) Tj ETQ Transactions, 2019, 48, 13074-13080.	q0 0 0 rgB 3.3	T /Overlock 7
87	Hydrogen Treatment for Superparamagnetic VO ₂ Nanowires with Large Roomâ€Temperature Magnetoresistance. Angewandte Chemie, 2016, 128, 8150-8154.	2.0	6
88	Magnetic origin of phase stability in cubic \hat{I}^3 -MoN. Applied Physics Letters, 2018, 113, 221901.	3.3	6
89	Reaction Pathways for α-Ga2O3 and β-Ga2O3 Phase Transition under Pressure up to 40 GPa: A First-Principles Study. Journal of Physical Chemistry C, 2020, 124, 23280-23286.	3.1	6
90	Atomic‣cale Characterization of Negative Differential Resistance in Ferroelectric Bi ₂ WO ₆ . Advanced Functional Materials, 2022, 32, 2105256.	14.9	6

#	Article	IF	CITATIONS
91	Two-Dimensional Layered Green Phosphorus as an Anode Material for Li-Ion Batteries. ACS Applied Energy Materials, 2022, 5, 2184-2191.	5.1	6
92	Coverage-dependent Orientations of Dy@C82Molecules on Au(111) Surface. Chinese Journal of Chemical Physics, 2012, 25, 423-428.	1.3	5
93	Reversible Potassium Intercalation in Blue Phosphorene–Au Network Driven by an Electric Field. Journal of Physical Chemistry Letters, 2020, 11, 5584-5590.	4.6	5
94	Hexamethoxytribenzocoronene, a Janus Double Concave Molecule to Selectively Assemble with Fullerene C60. Chemistry Letters, 2012, 41, 1588-1590.	1.3	4
95	Pauling's rules guided Monte Carlo search (PAMCARS): A shortcut of predicting inorganic crystal structures. Computer Physics Communications, 2020, 256, 107486.	7.5	4
96	Anisotropic black phosphorene nanotube anodes afford ultrafast kinetic rate or extra capacities for Li-ion batteries. Chinese Chemical Letters, 2022, 33, 3842-3848.	9.0	4
97	Dimerization of boron dopant in diamond (100) epitaxy induced by strong pair correlation on the surface. Journal of Physics Condensed Matter, 2013, 25, 045011.	1.8	3
98	Designing a Family of Aluminum-Containing Fluoroborate Crystals with Enhanced Birefringence and Second-Harmonic Generation Coefficients Based on the First-Principles Methods. Journal of Physical Chemistry C, 2021, 125, 7431-7438.	3.1	3
99	HSH-C10: A new quasi-2D carbon allotrope with a honeycomb-star-honeycomb lattice. Chinese Chemical Letters, 2021, , .	9.0	3
100	Ir Detectors: Ultrahigh Infrared Photoresponse from Core-Shell Single-Domain-VO2/V2O5Heterostructure in Nanobeam (Adv. Funct. Mater. 13/2014). Advanced Functional Materials, 2014, 24, 1820-1820.	14.9	2
101	Computational Study of a Novel 2D Ferromagnetic Metal: the Ce 2 C Monolayer. Physica Status Solidi - Rapid Research Letters, 2020, 14, 2000324.	2.4	2
102	A first-principles study on Al-doped ZnO growth polarity on sapphire (0001) surface. Europhysics Letters, 2016, 114, 66003.	2.0	1
103	Scanning Tunneling Spectroscopy of Metal Phthalocyanines on a Au(111) Surface with a Ni Tip. Chinese Physics Letters, 2011, 28, 076802.	3.3	0
104	Substrate engineering in stabilizing epitaxial MgO(1 1 1) polar ultrathin films: first-principles calculations. Journal of Physics Condensed Matter, 2014, 26, 315014.	1.8	0
105	Water Splitting: Strongly Coupled Nafion Molecules and Ordered Porous CdS Networks for Enhanced Visible-Light Photoelectrochemical Hydrogen Evolution (Adv. Mater. 24/2016). Advanced Materials, 2016, 28, 4943-4943.	21.0	0
106	Frontispiz: Supported Rhodium Catalysts for Ammonia–Borane Hydrolysis: Dependence of the Catalytic Activity on the Highest Occupied State of the Single Rhodium Atoms. Angewandte Chemie, 2017, 129, .	2.0	0
107	Frontispiece: Supported Rhodium Catalysts for Ammonia–Borane Hydrolysis: Dependence of the Catalytic Activity on the Highest Occupied State of the Single Rhodium Atoms. Angewandte Chemie - International Edition, 2017, 56, .	13.8	0